Quaternary Research **55**, 25–32 (2001)
doi:10.1006/qres.2000.2198, available online at http://www.idealibrary.com on IDEAL®

# Pacific Sea Surface Temperature Forcing Dominates Orbital Forcing of the Early Holocene Monsoon

Andrew Basil George Bush

*Department of Earth and Atmospheric Sciences, University of Alberta, 126 Earth Sciences Building, Edmonton, Alberta, Canada, T6G 2E3*

Received November 2, 1998

**Orbital forcing is known to play a primary role in regulating the strength of the south Asian monsoon circulation. In this study, a comparison is made between orbital forcing and Pacific sea surface temperature (SST) forcing of the monsoon through a sequence of atmospheric general circulation model experiments configured for 6,000 and 9,000 yr B.P. Early–mid Holocene orbital parameters are shown to increase continental seasonality as well as the meridional mean, the zonal mean, and the summer monsoon circulations. Winds in the southeast Asian monsoon are weakened by warm Pacific SST to such an extent that the increase in strength caused by early Holocene orbital parameters is offset. These results imply that SSTs are potentially as important as orbital parameters in governing the monsoon and that more data—particularly from the equatorial Pacific—are crucial to deciphering Holocene climate.**


*Key Words:* **Holocene climate; orbital forcing; SST forcing; El Niño.**

## INTRODUCTION

By virtually all indications, the south Asian summer monsoon in the early Holocene was stronger than it is today. A wealth of proxy data, assembled under the auspices of the COHMAP group and spanning the period from the last glacial maximum to the present, seem to consistently suggest that the early Holocene monsoon, in comparison to the present monsoon, exhibited increased winds along the Somali coast, increased Arabian Sea upwelling, higher lake levels, and higher rates of pollen deposition (see Wright *et al.* (1993) for a summary). Atmospheric general circulation model (GCM) calculations indicate that changes in the Earth's orbital parameters which amplify the seasonal cycle of incoming solar radiation—in particular, a hotter northern hemisphere summer—will intensify the south Asian summer monsoon (e.g., Kutzbach and Otto-Bliesner, 1982). The familiar and generally accepted picture which has emerged for the early Holocene is that increased obliquity and a summertime perihelion magnify the amplitude of the seasonal cycle, accentuating the land–sea temperature contrast and hence, through hydrostatic balance, the pressure gradient which is the fundamental driving force of the monsoon winds (e.g., Kutzbach and Guetter, 1984; Prell and Kutzbach, 1992).

Intriguing geoarchaeological data from coastal Peru and Ecuador indicate that the El Niño Southern Oscillation (ENSO) was absent for much of the early-mid Holocene between 11,000 and 5,000 yr B.P. (Rollins *et al.*, 1986; Sandweiss *et al.*, 1996). The absence of a Southern Oscillation is also suggested by pollen data from the southwest Pacific basin (Webb *et al.*, 1993a) and analyses of Peruvian ice cores (Thompson *et al.*, 1995). This suggests that the tropical Pacific Ocean was locked into one phase of ENSO or the other. Further, the data also suggest that relatively warm surface waters persisted off the west coast of South America north of 10°S throughout this period (although this may reflect a local warming rather than a warming of the entire eastern Pacific Ocean (DeVries and Wells, 1990; DeVries *et al.*, 1997)). Nevertheless, the level of Lake Titicaca was at a low stand in the early Holocene (COHMAP Members, 1994), a phenomenon which today occurs during El Niño events.

Both observations (e.g., Julian and Chervin, 1978) and atmospheric GCM calculations with imposed SST (e.g., Keshavamurty, 1982) have demonstrated that anomalously warm temperatures in the equatorial Pacific Ocean, such as those which occur during an El Niño event, significantly weaken the summer monsoon and bring relatively dry conditions to south Asia. During El Niño the locus of tropical convection shifts from the western Pacific to the central Pacific, enhancing subsidence over the west and bringing drier than normal conditions to eastern Australia, New Guinea, and the Indonesian islands (e.g., Peixoto and Oort, 1992). Increased surface divergence over the western Pacific induces anomalous surface easterlies over southern Asia and the Indian Ocean. These winds weaken the low-level westerly monsoon jet and reduce the moisture flux into, and the latent heat release over, the continental interior. While the dynamics involved in this monsoon/ENSO connection are still being unravelled (it is not exactly clear which process leads which), weak monsoons generally correlate with El Niño events and strong monsoons correlate with La Niña events (e.g., Rasmusson and Carpenter, 1982).

When taken together, the various proxy data for the early–mid Holocene seem to indicate a warm and tropical coastal Peru, above-average northwest Indian lake levels, and a strong south Asian monsoon. Are these data consistent with what is known about the impact of orbital parameters and SST on climate? In determining the strength of the south Asian monsoon, there appears



0033-5894/01 $35.00

to be a competition between two factors: early Holocene orbital forcing—which would increase the monsoon's strength—and the possibility of El Niño-like SST—which would decrease its strength. As the presence of the former forcing is well known from orbital calculations (e.g., Berger and Loutre, 1991) and the presence of the latter is suggested by some of the Holocene proxy data, it is necessary to quantify the relative impact of each in order to determine whether the climatic conditions implied by these data are self-consistent.

We performed a sequence of numerical simulations using GFDL's spectral atmospheric GCM (Gordon and Stern, 1982; Stone and Manabe, 1968; Wetherald and Manabe, 1988) at rhomboidal 30 truncation in the horizontal with 14 levels in the vertical. Seasonal solar insolation is imposed with the orbital parameters of obliquity, eccentricity, and longitude of perihelion set to the values computed for 9,000 and 6,000 yr B.P. (Berger, 1992). Ice sheet topography for 9,000 yr B.P. (Peltier, 1994) is imposed in the appropriate experiments after being spectrally decomposed with an isotropic spectral smoothing to reduce Gibbs oscillations (Navarra *et al.*, 1994). Monthly mean SSTs are interpolated to give daily values during the integration. With the exception of the 9,000 yr B.P. glaciers, bare surface albedos are set to modern values but may be altered during the course of the integration by snowfall. For the remnants of the Laurentide ice sheet, a glacial albedo of 0.6 is prescribed. The atmospheric carbon dioxide amount is set to 300 ppm in each experiment and is spatially uniform.

Two numerical experiments with different SST forcing were performed for each (6,000 and 9,000 yr B.P.) time slice. In the first set of experiments, present-day SST is prescribed (as determined from the Levitus (1982) data). In the second set of experiments a zonally uniform SST is imposed across the Pacific Ocean, with values determined from a zonal average of modern western Pacific SST between 144E and 167E; SST everywhere else is the same as in the first set of experiments (Fig. 1). The latter experiments are representative of a large El Niño event and provide an upper bound on the possible impact of Pacific SST forcing. We are not, in these sensitivity tests, proposing a mechanism whereby the mean thermocline depth may have increased; we are simply inferring what the climate would have been, given such an increase. A control simulation incorporating present-day SST, topography, and orbital parameters is performed to represent the "present-day" climate. Quantities in the following figures have been averaged over the last 3 years of the simulations.

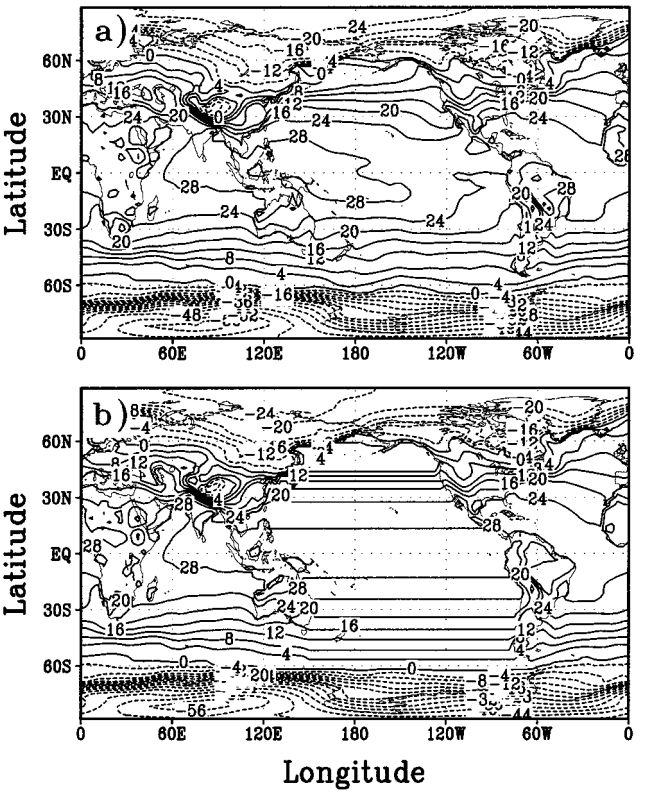


**FIG. 1.** Annual mean SST and (continental surface temperature) in °C for (a) modern SST (the first set of experiments) and (b)warm Pacific SST (second set of experiments).

## RESULTS WITH PRESENT-DAY SST

The spatial patterns of annual mean temperature anomalies are similar to those simulated in the COHMAP experiments and will therefore only be discussed briefly. Specifically, colder south Asian and north African winters and warmer Asian, European, and North American summers are common results (see Kutzbach *et al.*, 1993). The magnitudes of these changes are slightly larger here (presumably a result of the higher spectral resolution).

In the annual mean, enhanced wintertime cooling dominates summertime warming in most high-latitude regions because of the snow–albedo feedback. In both the 6,000 and the 9,000 yr B.P. simulations there is a spatial correlation of colder temperatures with increased snowfall, and of warmer temperatures with decreased snowfall. Colder winter temperatures in the early–mid Holocene are also consistent with results from the NCAR model (Bartlein *et al.*, 1998). The amplitude of the seasonal cycle is therefore larger than today over most of the Northern Hemisphere continental interiors in both the 6,000 and the 9,000 yr B.P. experiments.

More extensive snow cover in the Himalayas induces colder JJA temperatures in both experiments but does not weaken the summer monsoon. Consistent with previous results (e.g., Kutzbach and Otto-Bliesner, 1982; Prell and Kutzbach, 1992), early–mid Holocene orbital forcing increases the strength of the summer monsoon winds by approximately 18% in the 6,000 yr B.P. simulation and by 30% in the 9,000 yr B.P. simulation (Fig. 2; the Asian monsoon winds are the strong winds that blow along the east African coast then turn eastward over the Arabian Sea and India). Spatially averaged precipitation over the monsoon region (0N–40N; 50E–120E) increases by ~5% in the 6,000 yr B.P. simulation and by ~6% in the 9,000 yr B.P. simulation (see Fig. 6 below). The spatial locations of the precipitation maxima, however, are further west than they are today

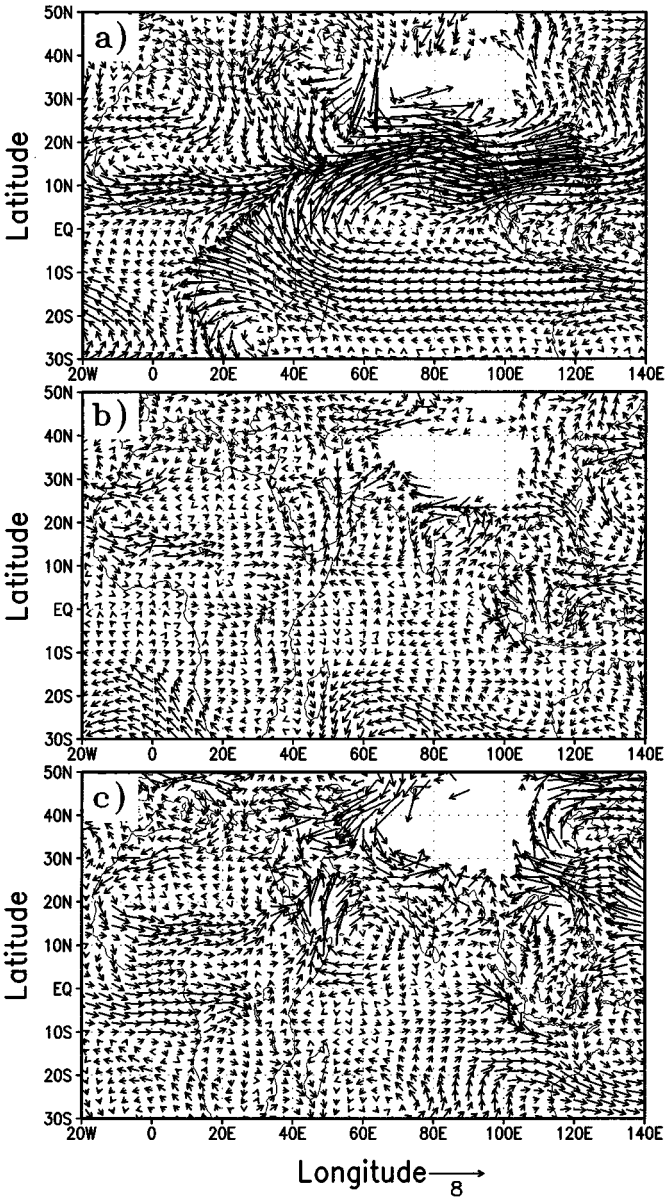


**FIG. 2.** (a) Simulated JJA 850 mb winds in the monsoon region of the present-day simulation. Vector differences in JJA 850 mb winds (experiment minus control) at (b) 6,000 yr B.P. and (c) 9,000 yr B.P. Units are m/s. Vectors in (b) and (c) are scaled as shown in the diagram, whereas vectors in (a) are scaled by twice the amount indicated.

since there is more northward inland penetration of the stronger southwesterly monsoon jet (cf. Fig. 2). This change in location of maximum orographic uplift leaves southwestern China and northeastern India drier than today.

Winds and precipitation in the westerly African summer monsoon are also increased in both Holocene experiments and lead to a near 100% increase in sub-Sahel precipitation between 10N and 15N. (see Fig. 7 below; the differences are greater at 9,000 yr B.P. than at 6,000 yr B.P. and have a larger spatial extent). The model employs a simple bucket soil moisture scheme and therefore does not have interactive vegetation, which is known to play a role in climatic feedbacks over the Sahara (e.g., Kutzbach *et al.*, 1996). The amount of precipitation north of 15N is therefore likely to be underestimated, but results for the sub-Sahel region are qualitatively consistent with those of Jolly *et al.* (1998).

The strength of the mean meridional circulation intensifies in both simulations, in agreement with results from the NCAR model (Kutzbach *et al.*, 1998). The Hadley cells are intensified by early Holocene orbital parameters, with both northern and southern hemisphere cells approximately 10% stronger than today at 6,000 yr B.P. The mean zonal circulation in the tropics also strengthens; the Pacific Walker circulation (which is an indicator of the strength of the equatorial easterlies) is stronger by approximately 10% at 6,000 yr B.P. and by 20% at 9,000 yr B.P. This strengthened global circulation is consistent with increased seasonality and increased thermal gradients driving stronger global winds.

## RESULTS WITH WARM EQUATORIAL PACIFIC SST

Anomalously warm SSTs in the central and eastern Pacific induce warmer annual mean temperatures over much of the tropical continents in both the 6,000 and the 9,000 yr B.P. experiments (Fig. 3). Latitudes poleward of 60N and 60S, however, retain

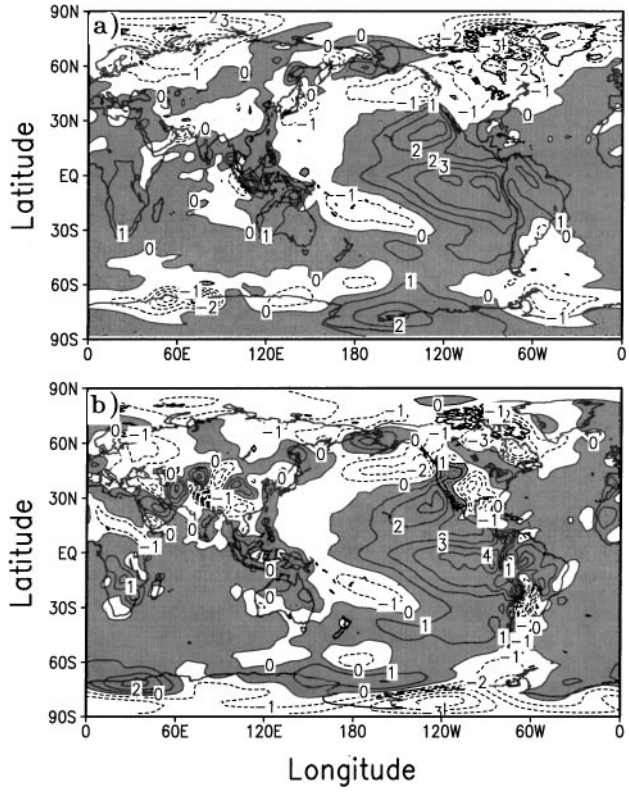


**FIG. 3.** Simulated departure of annual mean near surface temperature from modern values (°C) at (a) 6,000 yr B.P. and (b) 9,000 yr B.P. with warm Pacific SST imposed. The contour interval is 1°C in both panels. Darker shading indicates positive values and lighter shading indicates negative values.

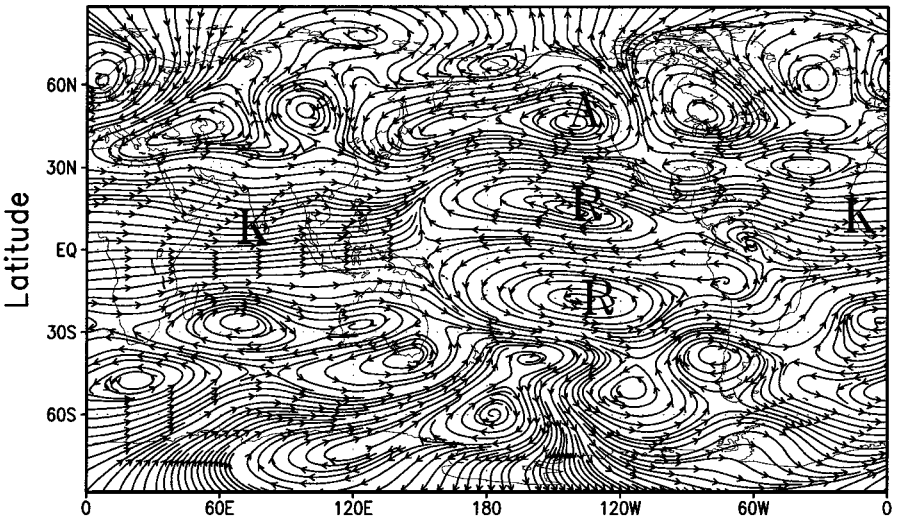


**FIG. 4.** Difference in upper tropospheric winds (plotted as a stream function) between the 9,000 yr B.P. experiments with warm Pacific SST and with modern SST. Arrows indicate the direction of wind differences. The atmosphere produces a Rossby wave response in the form of two tropical anticyclones (marked by *R*) and an equatorially symmetric Kelvin wave response (marked by *K*). The deepening of the Aleutian low (marked by *A*) is a consequence of the Rossby wave response (see text).

the same spatial pattern of cooling found in the present-day SST experiments. Warm temperatures over the eastern Pacific are a direct response to the imposed SST.

Two bands of cooling over the western Pacific (one extending southeast and one northeast from New Guinea) correlate spatially with a region of strong upper-level convergence and subsidence over longitudes 150E–180E (Fig. 4; shown for 9,000 yr B.P.). Two upper-tropospheric anticyclones are located above the SST anomaly. They constitute the tropical atmosphere's Rossby wave response to anomalously warm surface water. Upper-level westerly flow between South America and the Indonesian archipelago (a flow that is nearly symmetric about the equator) is the atmosphere's Kelvin wave response to the SST anomaly (see also Keshavamurthy (1982)). It is the interaction of these two flows that produces strong upper-level convergence and subsidence over the western Pacific, and thereby the anomalous easterly surface winds that modify the monsoon.

The anticyclonic circulations also weaken the upper tropospheric westerlies along the equator and intensify the westerly subtropical jets over the Pacific, phenomena which both occur during modern El Niño events (e.g., Hastenrath, 1996). Strengthening of the subtropical jet over the Pacific deepens the cyclonic Aleutian low (as marked by *A* in Fig. 4) and brings warmer winters to North America.

Tropical convection shifts from the western to the central Pacific, leaving higher than normal surface pressure over Indonesia. Along the equator, this high pressure produces an easterly wind anomaly over the Indian Ocean; off the equator, it produces anticyclonic circulations. This pattern is evident in the JJA 850 mb wind difference in the south Asian monsoon region (Fig. 5). The wind anomaly at 6,000 yr B.P. (Fig. 5a) is easterly across the entire north Indian Ocean and weakens the monsoon westerlies. Northeasterly anomalies along the African coast weaken the monsoon southwesterlies and reduce moisture flux onto the subcontinent. The response is stronger at 9,000 yr B.P. (Fig. 5b), with wind anomalies over the Indian Ocean typically 1 m/s stronger than at 6,000 yr B.P. Wind differences between the warm SST and modern SST simulations for 9,000 yr B.P. (Fig. 5c) indicate that the atmosphere's response to Pacific SST dominates its response to early–mid Holocene orbital parameters (because the wind difference pattern in Fig. 5c matches that in Fig. 5b).

A spatial average of JJA rainfall taken over the region between 50E–120E and 0N–40N indicates that, with modern SST, both the strength of the meridional winds and the area averaged precipitation increase (Fig. 6). With warm SST, however, summer monsoon precipitation is less than today by approximately 6% in the 6,000 yr B.P. simulation and by 5% in the 9,000 yr B.P. simulation. In addition, meridional wind speeds in the monsoon jet are weaker than today (Fig. 6c). (Also included in the figure, for comparison, are the results of a coupled atmosphere–ocean model for 6,000 yr B.P. which produced a strong monsoon (Bush, 1999).) The spatial distribution of anomalous precipitation is correlated with changes in monsoon winds. Despite the fact that the monsoon is weaker overall, some regions in northwestern India have increased precipitation where anomalous westerlies near 30N are orographically uplifted (cf. Fig. 5).

With warm SST, the mean Hadley circulation is stronger (not shown) because it must transport more heat out of the equatorial region. Differences in the annual mean Walker circulation, however, show a marked 70% reduction in easterly trade wind strength over the central–eastern Pacific. The winds decrease because the difference in pressure between the eastern and western Pacific is much smaller. (With modern SST there is high pressure over the eastern Pacific and low pressure over the western Pacific and hence strong easterly surface winds). Changes in the

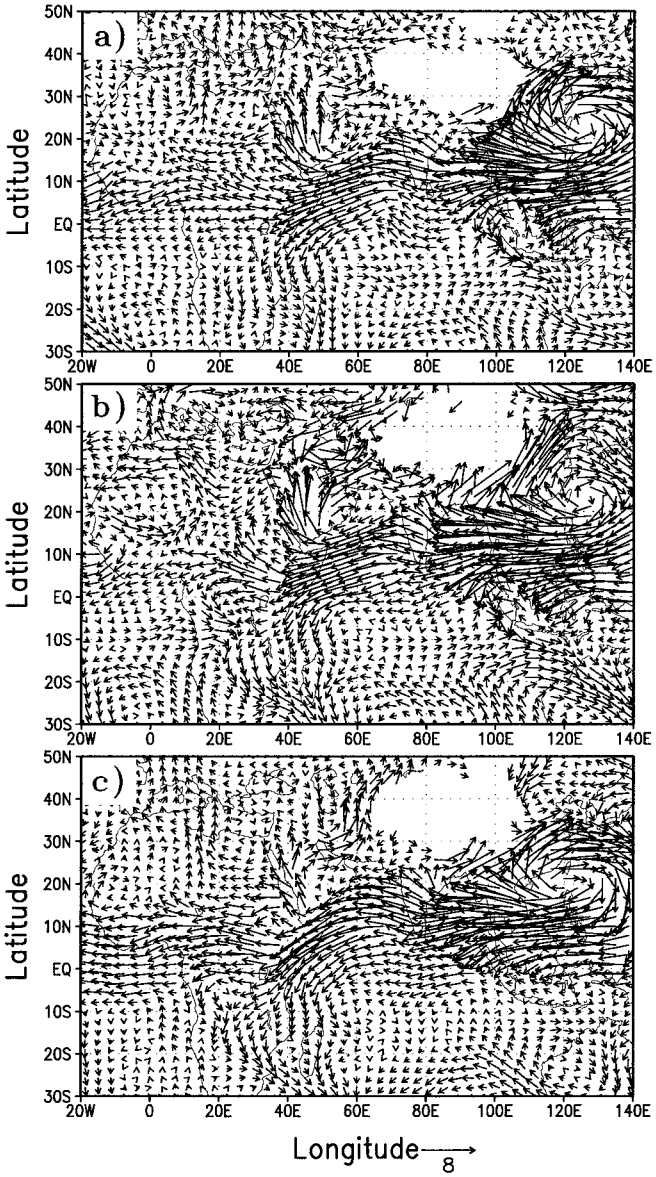


**FIG. 5.** Vector wind differences in JJA 850 mb winds in the monsoon region for (a) 6,000 yr B.P. and (b) 9,000 yr B.P. with warm Pacific SST. Part (c) shows the 9,000 yr B.P. difference between the experiment with warm Pacific SST and modern SST. Units are m/s, and vectors are scaled as shown in the diagram.

annual mean tropical circulations are therefore dominated by the atmosphere's response to warm SST rather than its response to the orbital parameters.

## DISCUSSION AND CONCLUSIONS

The similarity between the results of the first set of experiments—in which the atmosphere is forced by modern SST—and those of previous studies (e.g., Wright *et al.*, 1993; Kutzbach *et al.*, 1998) indicates that numerical simulations of early–mid Holocene climate generate robust climatic signatures which are fairly model independent. For example, a stronger seasonal cycle, stronger monsoon winds, increased monsoon precipitation, and stronger tropical circulations are all common results that arise from changes in the Earth's orbital forcing.

The second set of experiments demonstrates that SST forcing by anomalously warm central and eastern Pacific water can dominate orbital forcing in many of these atmospheric responses. In particular, the south Asian monsoon in both the 6,000 and the 9,000 yr B.P. simulations is weaker than it is today (cf. Fig. 6). In addition, the global circulation changes in such a way as to deepen the Aleutian low and to bring warmer winters to the North

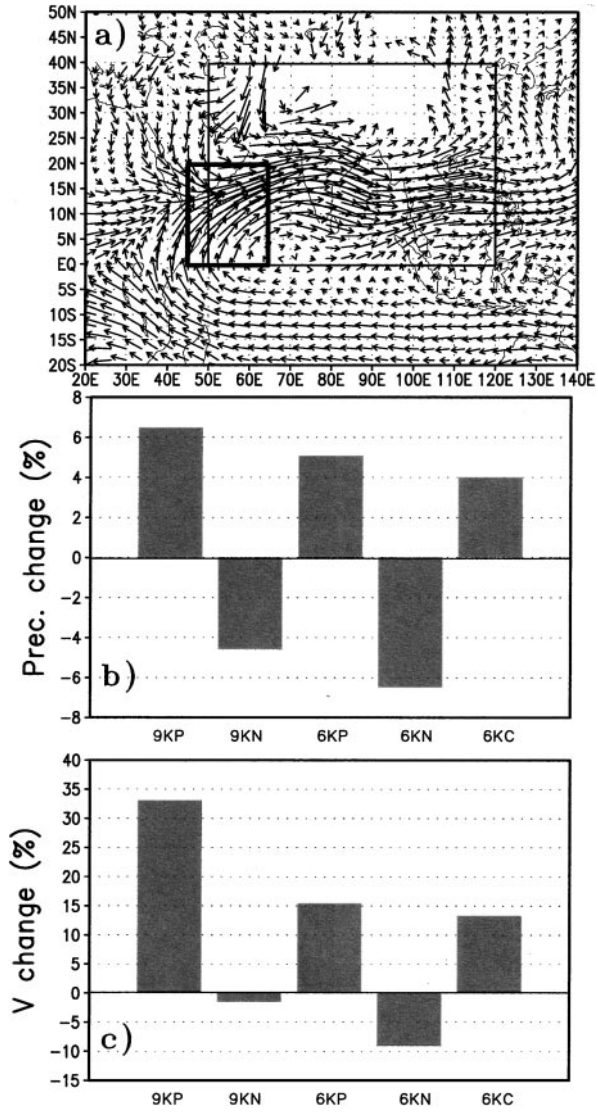


**FIG. 6.** Percentage changes (from the present-day simulation) of JJA mean (b) precipitation and (c) meridional velocity for all experiments. Spatial averaging for precipitation is taken over the rectangular region indicated by the thin line in (a), and for meridional velocity it is taken over the region indicated by the thick line in (a). Acronyms for the experiments are listed underneath their respective bars and are denoted by 9K for the 9,000 yr B.P. experiments and 6K for the 6,000 yr B.P. experiments, with the suffixes P (present day SST) and N (warm Pacific SST). Also included are the results from the coupled model simulation of Bush (1999), denoted as 6KC.

American interior, a result that is in much better agreement with the pollen data (Webb *et al.*, 1993b).

The second set of experiments also demonstrates that changes in the spatial distribution of rainfall in northern India do not necessarily correlate with changes in monsoon wind speeds. Changes in monsoon wind *direction* can also produce positive precipitation anomalies across large regions even though the monsoon is, on average, weaker. Changes in the monsoon circulation pattern itself should therefore be considered when interpreting lake level data from this region.

In contrast to the Asian monsoon region, orbital forcing appears to be dominant in governing moisture flux over the African monsoon region since the percentage changes in precipitation and soil moisture are dominated by the orbital response (Fig. 7).

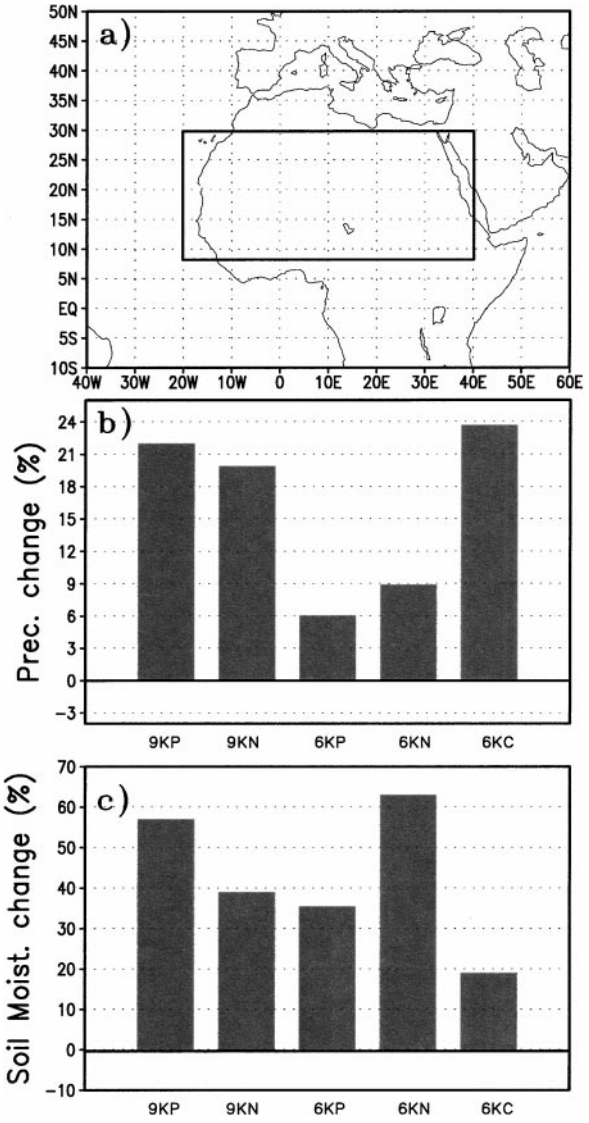


**FIG. 7.** Percentage changes (from the present-day simulation) of annual mean (b) precipitation and (c) soil moisture averaged over the region indicated in (a) for all experiments. Acronyms are the same as in Figure 6.

Warm Pacific SST, however, does increase Sahel and Saharan soil moisture in both the 6,000 and the 9,000 yr B.P. simulations, indicating that the SST response is in phase with that of the orbital forcing in this part of the world.

In comparing these results to the evidence from coastal Peru for warm SST south of the equator (Sandweiss *et al.*, 1996), we can conclude that the magnitude of a persistent warm SST event could not have been as large as in our experiments. Otherwise they would have weakened the south Asian monsoon, a result that does not concur with the marine record of enhanced upwelling (Prell, 1984). A second possibility is that the cold tongue was indeed present in the early Holocene but that SST to the south warmed regionally. Such a phenomenon could occur if there were a reduction of marine stratus clouds off the Peruvian coast, clouds that are today responsible for maintaining cold SST south of the equator (Philander *et al.*, 1995) and that may have been reduced in a climate with increased seasonality. If inferences can be made from proxy data about the conditions of the seasonal cycle in the eastern equatorial Pacific, then the issue of whether the climate was in a semipermanent El Niño or La Niña state may be resolved. Current uncertainty regarding early–mid Holocene SST, combined with the magnitude of the climatic impact that Pacific SST can have, as demonstrated here, suggests that it is vital to obtain accurate SST reconstructions for this time period.

While sensitivity tests such as these provide valuable information on the range of possibilities in the climate system, an inconsistency nevertheless exists in comparing proxy data to simulated climates which differ from today's and yet are forced by modern SST. If the mean temperature and wind velocity in the atmosphere are different, as is the case in the first set of experiments, then the mean state of the ocean would also be different. That the atmosphere–ocean system would adjust itself to deliver a climate that resembles what is seen in an atmosphere-only integration forced by modern SST is unlikely. Recent simulations using coupled atmosphere–ocean models indicate that La Niña-like conditions were probable in the mid-Holocene (Bush, 1999) but that the Pacific still exhibited interannual variability (Otto-Bleisner, 1999). Nevertheless, coupled model studies are sensitive to the initial depth of the Pacific thermocline. To demonstrate that a warm tropical Pacific is, in fact, a possible scenario, a coupled model (same as in Bush (1999)) configured for today is used to determine what the Pacific SST would be if the thermocline were everywhere as deep as in the western Pacific. After 8 years of integration, the thermocline in the east is sufficiently deep that the trade winds cannot upwell it to the surface; permanently warm SSTs therefore persist throughout the integration (Fig. 8). If there is a dynamical mechanism to deepen the thermocline in the east sufficiently, warm SSTs will persist. Decadal, centennial, and, perhaps, millennial climate variability are likely candidates for inducing long time scale thermocline depth anomalies. Longer integrations of high-resolution coupled models are necessary in order to further explore this possibility.

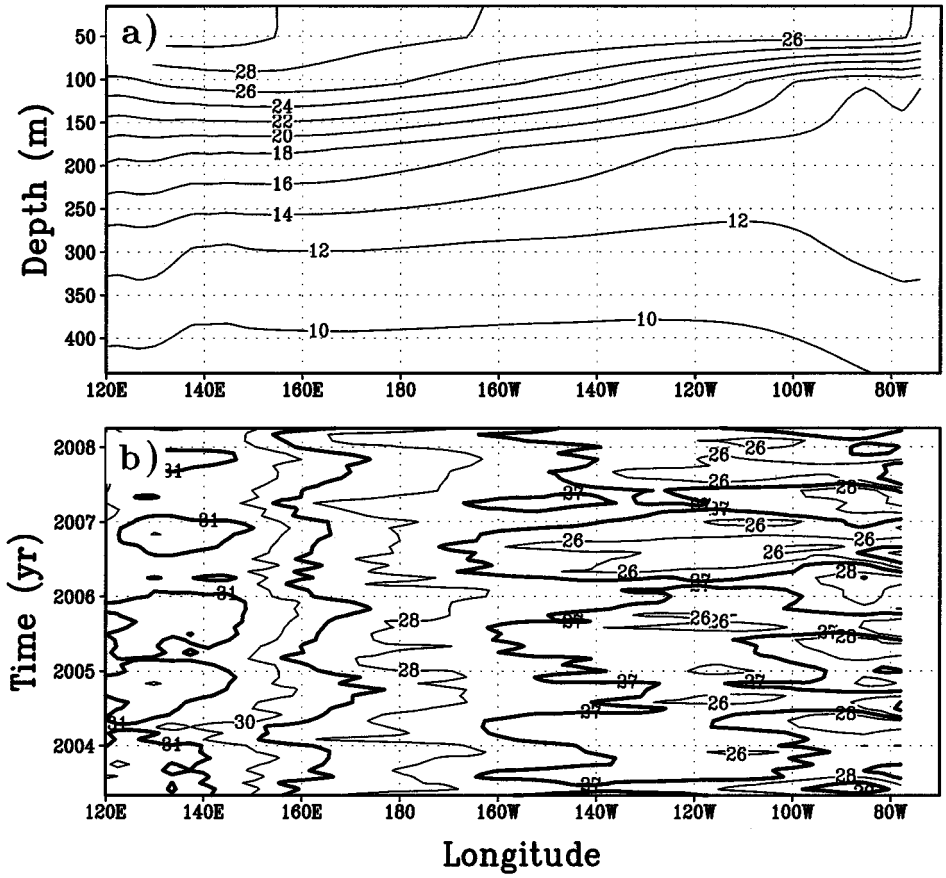


**FIG. 8.** Results from a coupled atmosphere–ocean general circulation model initialized with a deep Pacific thermocline (see text). (a) Equatorial Pacific Ocean temperature (as a function of depth) averaged over the last 3 years of the integration (c.i. 2°C), and (b) Pacific Ocean SST as a function of time for the last 5 years of the simulation (c.i. 1°C; every other isotherm has been thickened for clarity).

## ACKNOWLEDGMENTS

The author thanks the Natural Sciences and Engineering Research Council for support through Research Grant OGP0194151 and the Climate System History and Dynamics Project, as well as UNESCO for sponsoring International Geological Correlation Project 415.

## REFERENCES

Bartlein, P. J., Anderson, K. H., Anderson, P. M., Edwards, M. E., Mock, C. J., Thompson, R. S., Webb, R. S., Webb, T., III, and Whitlock, C. (1998). Paleoclimate simulations for North America over the past 21,000 years: Features of the simulated climate and comparisons with paleoenvironmental data. *Quaternary Sciences Review* **17,** 549–585.

Berger, A. (1992). Orbital Variations and Insolation Database. IGB.P. PAGES/World Data Center-A for Paleoclimatology Data Contribution Series No. 92-007. NOAA/N GDC Paleoclimatology Program, Boulder, CO.

Berger, A., and Loutre, M. F. (1991). Insolation values for the climate of the last 10 million years. *Quaternary Sciences Review* **10**(4), 291–317.

Bush, A. B. G. (1999). Assessing the impact of mid-Holocene insolation on the atmosphere–ocean system. *Geophysical Research Letters* **26,** 99–102.

COHMAP Members (1994). Oxford Lake Levels Database. IGBP PAGES/ World Data Center-A for Paleoclimatology Data Contribution Series No. 94-028. NOAA/NGDC Paleoclimatology Program, Boulder, Co.

DeVries, T. J., and Wells, L. E. (1990). Thermally anomalous Holocene molluscan assemblages from coastal Peru: Evidence for paleogeographic, not climatic, change. *Palaeogeography, Palaeoclimatology, Palaeoecology* **81,** 11–32.

DeVries, T. J., Ortlieb, L., Diaz, A., Wells, L., Hillaire-Marcel, C., Wells, L. E., Noller, J. S., Sandweiss, D. H., Richardson, J. B., III, Reitz, E. J., Rollins, H. B., Maasch, K. A. (1997). Determining the early history of El Niño. *Science* **276,** 965.

Gordon, C. T., and Stern, W. (1982). A description of the GFDL global spectral model. *Monthly Weather Review* **110,** 625–644.

Hastenrath, S. (1996). "Climate Dynamics of the Tropics," pp. 273–288. Kluwer Academic, Dordrecht.

Julian, P. R., and Chervin, R. M. (1978). A study of the Southern Oscillation and Walker circulation phenomenon. *Monthly Weather Review* **106,** 1433–1451.

Jolly, D., Harrison, S. P., Damnati, B., and Bonnefille, R. (1998). Simulated climate and biomes of Africa during the late Quaternary: Comparison with pollen and lake status data. *Quaternary Science Reviews* **17,** 629–657.

Keshavamurty, R. N. (1982). Response of the atmosphere to sea surface temperature anomalies over the equatorial Pacific and the teleconnections of the Southern Oscillation. *Journal of the Atmospheric Sciences* **39,** 1241–1259.

Kutzbach, J. E., and Guetter, P. J. (1984). The sesitivity of monsoon climates to orbital parameter changes for 9000 years B.P.: Experiments with the NCAR general circulation model. *In* "Milankovitch and Climate" (A. Berger, J. Imbrie, J. D. Hays, G. J. Kukla, and B. Saltzman, Eds.), pp. 801–820. Reidel, Dordrecht.

Kutzbach, J. E., and Otto-Bliesner, B. L. (1982). The sensitivity of the African–Asian monsoonal climate to orbital parameter changes for 9000 years B.P. in a low-resolution general circulation model. *Journal of the Atmospheric Sciences* **39,** 1177–1188.

Kutzbach, J. E., Guetter, P. J., Behling, P. J., and Selin, R. (1993). Simulated climatic changes: Results of the COHMAP climate-model experiments. *In* "Global Climates since the Last Glacial Maximum" (H. E. Wright, Jr., J. E. Kutzbach, T. Webb III, W. F. Ruddiman, F. A. Street-Perrott, and P. J. Bartlein, Eds.), pp. 24–93. Univ. of Minnesota Press, Minneapolis.

Kutzbach, J. E., Bonan, G., Foley, J., and Harrison, S. P. (1996). Vegetation and soil feedbacks on the response of the African monsoon to orbital forcing in the early to middle Holocene. *Nature* **384,** 623–626.

Kutzbach, J. E., Gallimore, R., Harrison, S., Behling, P., Selin, R., and Laarif, F. (1998). Climate and biome simulations for the past 21,000 years. *Quaternary Science Reviews* **17,** 473–506.

Levitus, S. (1982). "Climatological Atlas of the World Ocean," NOAA Prof. Paper 13. U.S. Govt. Printing Office, Washington, DC.

Navarra, A., Stern, W. F., and Miyakoda, K. (1994). Reduction of the Gibbs oscillation in spectral model simulations. *Journal of Climate* **7,** 1169–1183.

Otto-Bleisner, B. L. (1999). El Niño/La Niña and Sahel precipitation during the middle Holocene. *Geophysical Research Letters* **26,** 87–90.

Peixoto, J. P., and Oort, A. H. (1992). "Physics of Climate." Am. Inst. of Phys., New York.

Peltier, W. R. (1994). Ice age paleotopography. *Science* **265,** 195–201.

Philander, S. G. H., Gu, D., Halpern, D., Lambert, G., Lau, N.-C., Li, T., and Pacanowski, R. C. (1995). Why the ITCZ is mostly north of the equator. *Journal of Climate* **9,** 2958–2972.

Prell, W. L. (1984). Monsoonal climate of the Arabian Sea during the late Quaternary: A response to changing solar radiation. *In* "Milankovitch and Climate" (A. Berger *et al.*, Eds.), pp. 349–366. Reidel, Dordrecht.

Prell, W. L., and Kutzbach, J. E. (1992). Sensitivity of the Indian monsoon to forcing parameters and implications for its evolution. *Nature* **360,** 647–652.

Rasmusson, E. M., and Carpenter, T. H. (1982). The relationship between eastern equatorial Pacific sea surface temperatures and summer monsoon rainfall over India and Sri Lanka. *Monthly Weather Review* **111,** 517–528.

Rollins, H. B., Richardson, J. B., III, Sandweiss, D. H. (1986). The birth of El Niño: Geoarchaeological evidence and implications. *Geoarchaeology: An International Journal* **1,** 3–15.

Sandweiss, D. H., Richardson, J. B., III, Reitz, E. J., Rollins, H. B., and Maasch, K. A. (1996). Geoarchaeological evidence from Peru for a 5000 years B.P. onset of El Niño. *Science* **273,** 1531–1533.

Stone, H. M., and Manabe, S. (1968). Comparisons among various numerical models for computing infrared cooling. *Monthly Weather Review* **96,** 735–741.

Thompson, L. G., Mosley-Thompson, E., Davis, M. E., Lin, P.-N., Henderson, K. A., Cole-Dai, J., Bolzan, J. F., and Liu, K.-B. (1995). Late glacial stage and Holocene tropical ice core records from Huascarán, Peru. *Science* **269,** 46–50.

Webb, T., III, Ruddiman, W. F., Street-Perrott, F. A., Markgraf, V., Kutzbach, J. E., Bartlein, P. J., Wright, H. E., Jr., and Prell, W. L. (1993a). Climatic changes during the past 18,000 years: Regional syntheses, mechanisms, and causes. *In* "Global Climates since the Last Glacial Maximum" (H. E. Wright, Jr., J. E. Kutzbach, T. Webb III, W. F. Ruddiman, F. A. Street-Perrott, and P. J. Bartlein, Eds.), pp. 514–535. Univ. of Minnesota Press, Minneapolis.

Webb, T., III, Bartlein, P. J., Harrison, S. P., and Anderson, K. H. (1993b). Vegetation, lake levels, and climate in eastern North America for the past 18,000 years. *In* "Global Climates since the Last Glacial Maximum" (H. E. Wright, Jr., J. E. Kutzbach, T. Webb III, W. F. Ruddiman, F. A. Street-Perrott, and P. J. Bartlein, Eds.), pp. 415–467. Univ. of Minnesota Press, Minneapolis.

Wetherald, R. W., and Manabe, S. (1988). Cloud feedback processes in a general circulation model. *Journal of the Atmospheric Sciences* **45,** 1397–1415.

Wright, H. E., Jr., Kutzbach, J. E., Webb, T., III, Ruddiman, W. F., Street-Perrott, F. A., and Bartlein, P. J., Eds. (1993). "Global Climates since the Last Glacial Maximum." Univ. of Minnesota Press, Minneapolis.